



Memo 117

Focal Plane Array Simulations with MeqTrees II: Noise Analysis

A. Gray

A.G. Willis

09/09

Focal Plane Array Simulations with MeqTrees II: Noise Analysis

A. Gray & A.G. Willis
National Research Council Canada
Herzberg Institute of Astrophysics
Dominion Radio Astrophysical Observatory
Penticton, BC, V2A 6J9, Canada
Andrew.Gray@nrc-cnrc.gc.ca

September 25, 2009

1 Introduction

In a previous memo [1] we demonstrated the use of the MeqTrees simulation package [2] to compare the results of three different beam forming techniques for phased-array feeds (PAFs): conjugate field matching (CFM), Gaussian fitting, and fitting to a GRASP-designed feed. Here we apply the methods discussed in that memo to study the noise distributions expected in synthesis images made from telescopes equipped with PAFs.

There are two aspects to this work, looking at how noise in the final images is affected by (1) different beam forming techniques, and (2) noise correlation in overlapping beams arising from the re-use of signals from the array elements in forming each beam. Note that the latter effect is distinct from the phenomenon of noise coupling between array elements, which we do not consider here.

2 Making Noise Images

To make images, we used MeqTrees to simulate an interferometer with 30 identical antennas, each equipped with an identical 9×10 PAF. Each element in each PAF was given a unique random noise signal. No sky signal or signal due to coupling between elements was included.

A MeqTrees script was used to generate a measurement set by applying the appropriate element weights to each PAF element to form the desired beam, and then forming visibilities between all antenna pairs (as described in [1]). This was repeated for each offset beam position, using the same random noise signals per element. The measurement sets so produced were then imaged using the AIPS++ imager, producing FITS images for each beam.

This process was repeated for both CFM and Gaussian weighting schemes.

3 Comparison of Weighting Schemes

To measure the noise in the images, the final FITS images were read into the DRAO MADR reduction package and the rms of each was obtained with the EXT function. The results are shown in Figure 1.

In both CFM and Gaussian cases the rms increases slowly with increasing PAF beam offset from bore-sight over much of the range considered. This is caused by the finite size of the array, with fewer elements participating in the offset beams as offset increases. The sharper rise seen around 3 times FWHM indicates that the focal spot is starting to move off the edge of the array.

In the Gaussian case there are also fluctuations in the rms at smaller offsets, probably caused by variations in the fitting process. The limited number of elements available for the fit at large offsets also results in a dramatic rise in the rms.

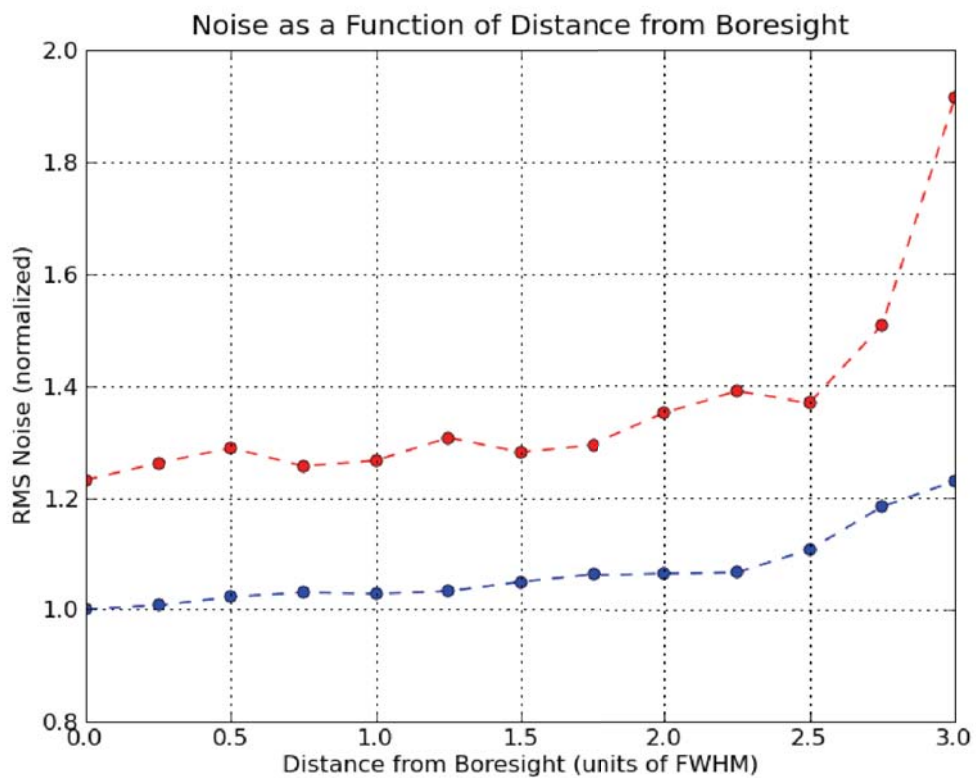


Figure 1: Observed noise as a function of PAF beam offset relative to the bore-sight. The blue points plot the noise observed in images made using the CFM weighting scheme, while the red points plot the noise from images made using Gaussian weights.

These variations aside, the noise is generally about 20 percent higher in the images made with a Gaussian weighting during beam formation versus those made using CFM. An examination of the weights derived in the two cases (e.g., Figure 2) shows that this happens because the Gaussian fitting assigns larger weights to a smaller number of PAF elements in the proximity of the focal spot.

To illustrate this more clearly, Figure 3 shows the result of dividing the complex CFM weights by the amplitude of the corresponding Gaussian weights. There is clearly a larger relative weight contribution from the CFM weights at large distances from the phase-up position.

4 Noise Correlation

4.1 Correlation Between Array Beams

To assess the noise correlation between the array beams themselves, each offset image was averaged pixel-wise (i.e., not in their correct relative spatial locations) with the on-axis beam image, and the rms over all pixels calculated and compared with the value expected if the noise was independent. The resulting relative rms noise as a function of beam offset is shown in Figure 4. This process was repeated using the 1 FWHM offset position as reference, yielding the result in Figure 5. The result here is clearly consistent with the on-axis case, as expected.

Both cases show that noise in adjacent beams is correlated on the scale of a beam. This merely tells us that independent beams are generated by independent array elements; i.e., ones at least a focal-spot diameter apart.

4.2 Correlation in Mosaiced Noise Images

For this part of the study the on-axis (0 FWHM) and 1 FWHM offset images were used in their correct relative spatial positions, and “mosaiced” together to form a wide-field image using the DRAO `supertile` program. The resulting rms noise as a function of position along the line joining the field centres is shown in Figure 6. Note that no primary beam correction was applied to the data, so the noise is ‘flat’ across the field.

Clearly, the region of the overlap between fields ($\pm 55'$) exhibits the rms expected for independent noise. Note that the field at 1 FWHM (at right in Figure 6) has a slightly higher noise, consistent with the results discussed earlier.

5 Discussion

While adjacent phased array beams use common array elements, noise correlation is not an issue for interferometric imaging. This is because the the phase rotations inherent in interferometric imaging decorrelate the noise. While the noise in individual pixels does correlate when examined pixel-for-pixel, when added with appropriate spatial offsets to properly image the sky, the pixels are no longer coincident and the correlation disappears. Note that the exceptional case of having two or more PAF beams separated by less than a few pixels will still show noise correlation in the overlapped image, but this scenario is unlikely to occur in reality.

While noise correlation is not an issue for noise amplitude in the overlap between interferometer fields, there will still be correlations in the noise in areas of sky separated by the beam spacing, because the noise pattern projected on to the sky is common for adjacent beams. Since many of the science goals for instruments likely to be equipped with PAFs are survey oriented, this limitation may be significant when studying weak populations over such scales, or for single-antenna PAF applications.

Since different weighting schemes lead to quite different noise levels in synthesized images, we suggest that there is no such thing as a ‘best’ weighting scheme. Surveys where the goal is the detection of faint objects may choose to use something similar to conjugate weighting even though the beam shape is not optimal [1]. Surveys requiring many overlapping fields and a well-shaped beam may elect to use a weighting scheme that produces a such a beam at the expense of increased noise.

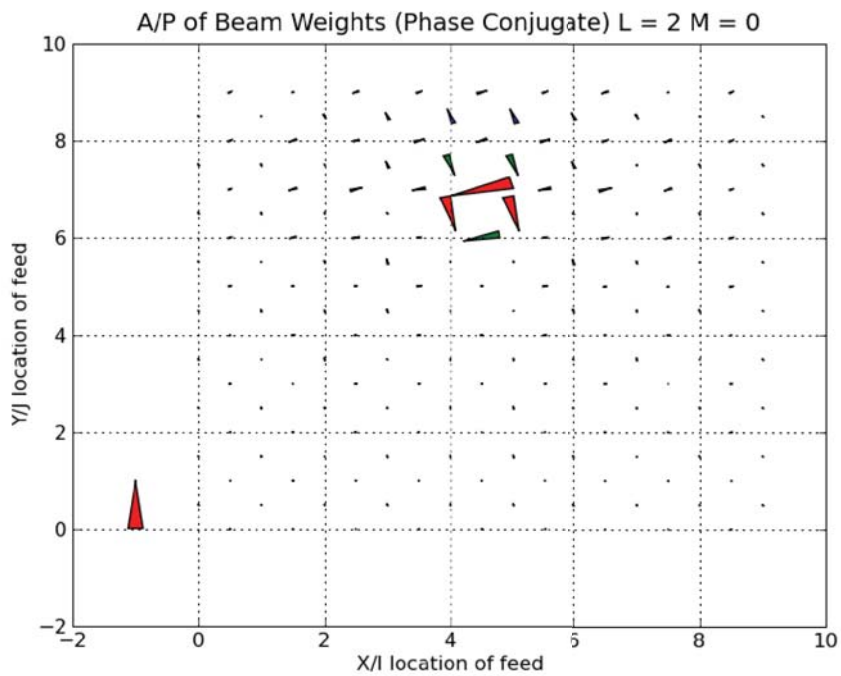
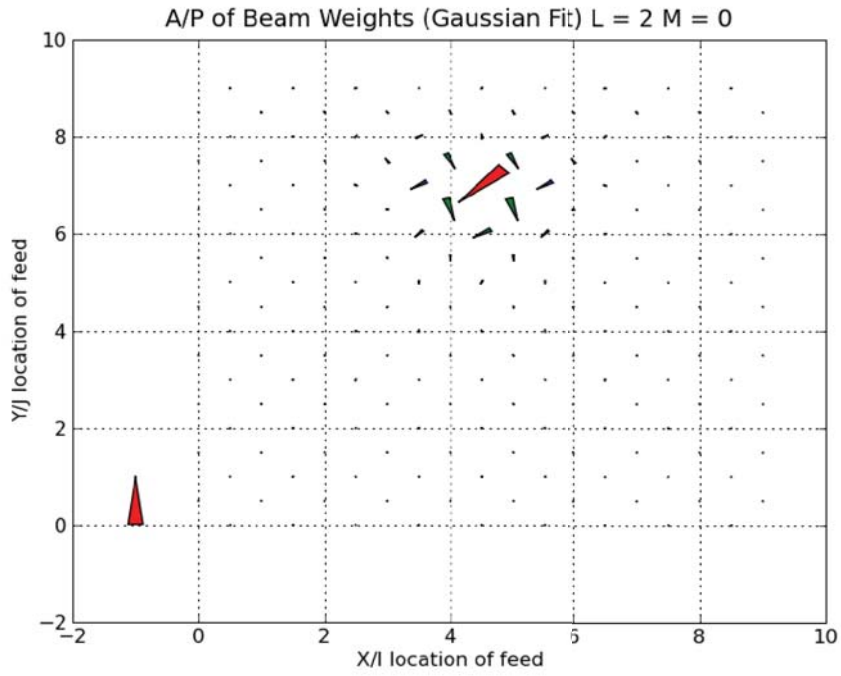


Figure 2: The difference in weighting emphasis for a phased-up beam at $L=2$, $M=0$ (see Memo xx).

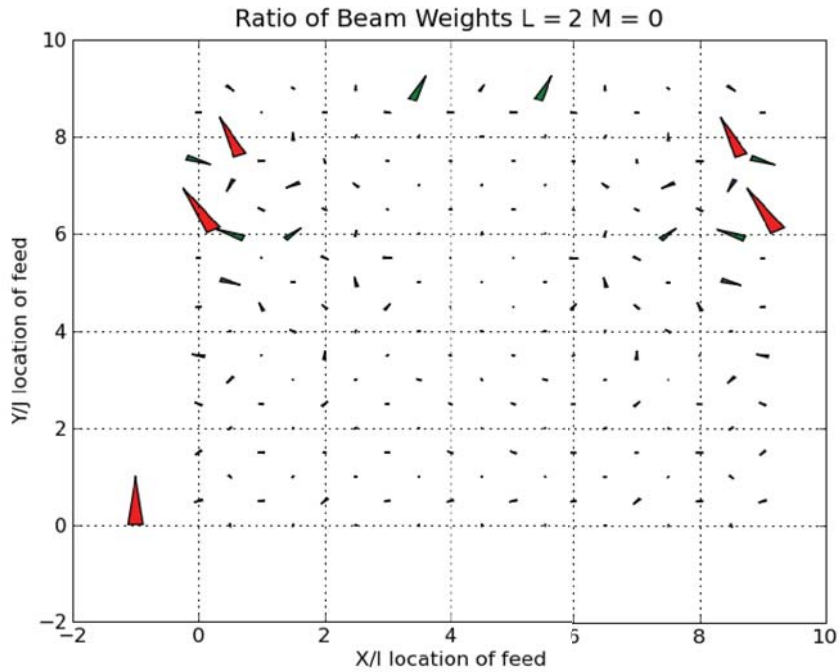


Figure 3: Same data as Figure 2, with the complex CFM weights divided by the amplitude of the Gaussian weights, showing that CFM weights are larger at greater distance from the focal spot.

References

- [1] A. G. Willis, B. Veidt, and A. Gray, “SKA memo 115 Focal Plane Array Simulations with Meqtrees 1:Beamforming,” International SKA Project Office, Tech. Rep., 2009. [Online]. Available: <http://www.skatelescope.org/PDF>
- [2] J. E. Noordam and O. M. Smirnov, “Meqtrees: A software module for implementing an arbitrary Measurement Equation and solving for its parameters,” *In Preparation*, 2009.

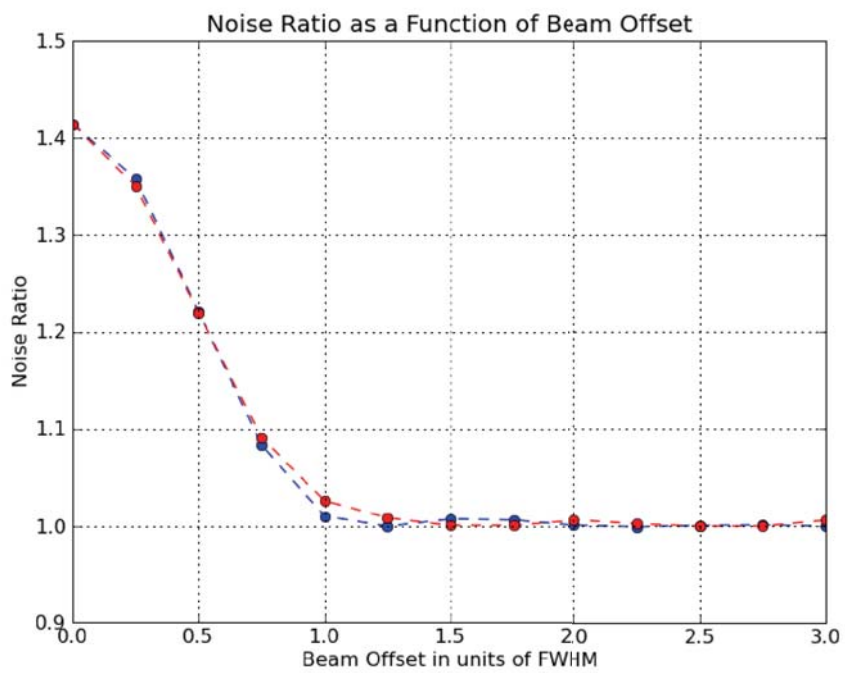


Figure 4: Ratio of noise observed in averaged fields to the noise expected if the data were independent, as a function of PAF beam offset, using the zero offset position as reference. The blue points plot the noise made from a PAF using CFM weighting while the red points plot the noise with an PAF using Gaussian weights.

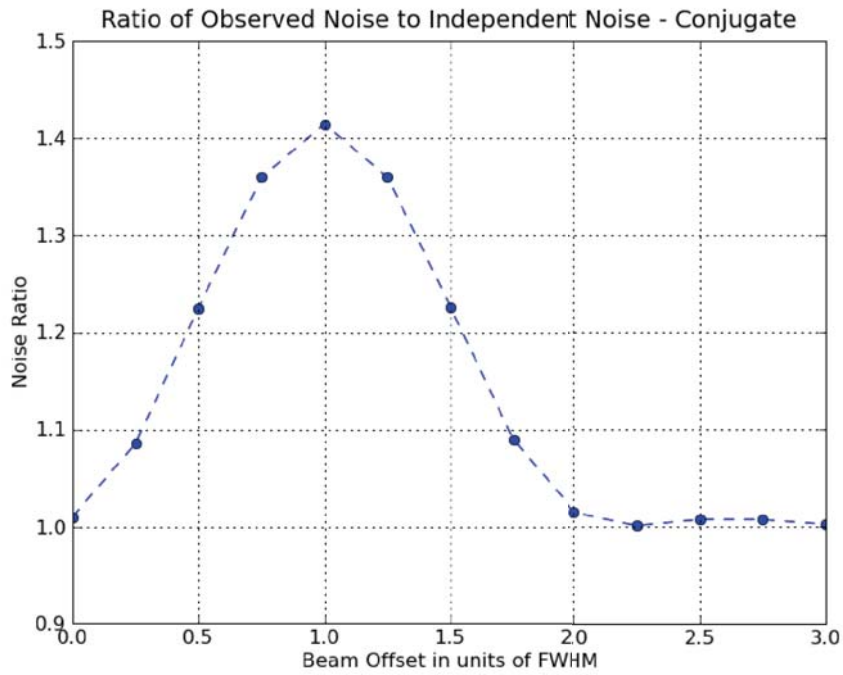


Figure 5: Ratio of noise observed in averaged fields to the noise expected if the data were independent, as a function of PAF beam offset, using the 1 FWHM offset position as reference (only CFM weighting shown).

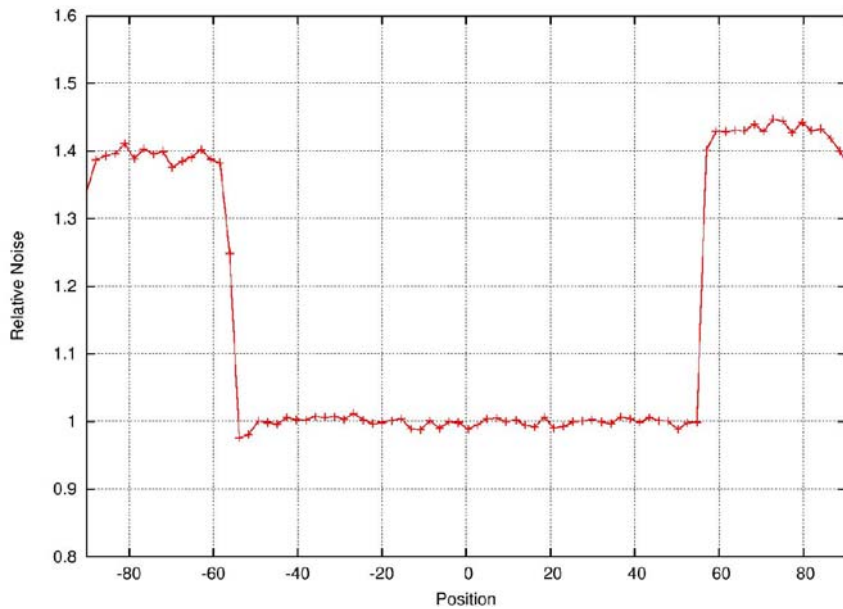


Figure 6: Relative noise in mosaiced images from adjacent, overlapping PAF beams (overlap region from $-55'$ to $+55'$). The on-axis beam is at left; note that the offset beam has higher noise, as seen previously.